Chiroptical Phenomena in Reverse Micelles: The Case of (1*R*,2*S*)-Dodecyl (2-hydroxy-1-methyl-2-phenylethyl)dimethylammonium Bromide (DMEB)

SERGIO ABBATE,[1,2]* MARCO PASSARELLO,[1,3] FRANCE LEBON,[1,2] GIOVANNA LONGHI,[1,2] ANGELA RUGGIRELLO,[4,5] VINCENZO TURCO LIVERI,[4,5] FIORENZA VIANI,[6] FRANCA CASTIGLIONE,[3] DANIELE MENDOLA,[3] AND ANDREA MELE[3,6]

[1]*Dipartimento di Medicina Molecolare e Traslazionale, Università di Brescia, Brescia, Italy*
[2]*Consorzio Interuniversitario Scienze Fisiche della Materia, Roma, Italy*
[3]*Department of Chemistry, Materials and Chemical Engineering "G. Natta," Politecnico di Milano, Milano, Italy*
[4]*Dipartimento di Chimica, Università degli Studi di Palermo, Palermo, Italy*
[5]*ISMN, Istituto per lo Studio dei Materiali Nanostrutturati, Palermo, Italy*
[6]*Istituto di Chimica del Riconoscimento Molecolare - CNR, Milano, Italy*

INTRODUCTION

The search of new surfactant molecules and the characterization of new and old surfactants is an active research goal and a technology-driven activity.[1] Within this field particular attention is paid to chiral biosurfactants,[2,3] and to their ability of selectively associating with other molecules through a mechanism that we may generically refer to as chiral recognition.[3,4] (1*R*,2*S*)-Dodecyl(2-hydroxy-1-methyl-2-phenylethyl) dimethylammonium bromide (DMEB) is a commercial cationic single-tailed surfactant whose molecular structure, shown in the right part of Scheme 1, is characterized by a chiral and biologically active head group (a positively charged ephedrine moiety with a quaternary ammonium group) covalently bound to an hydrophobic dodecyl chain. The phenylalkyl group carries two stereogenic centers and the OH group can form intermolecular hydrogen bonds.

These structural features, joined to the ability to form direct micelles and giant vesicles in water,[5,6] have already been exploited in the production of surfactant-templated chiral mesoporous sol-gel materials,[7,8] the recognition and separation of racemic mixtures,[4,9–11] and the synthesis of chiral compounds.[12,13] However, to the best of our knowledge, no attempt to investigate the self-assembling capability of this surfactant in apolar media has been carried out up to now despite the remarkable theoretical and practical importance of surfactant aggregates—reverse micelles—, in such environments. In fact, these aggregates have found many interesting applications, like the confinement of water and other hydrophilic molecules within their core,[14,15] the influence on reaction rates and mechanisms,[16] and the possibility of synthesizing a wide variety of nanoparticles with fine size-control.[17]

In the case of DMEB reverse micelles, further specific applications, which are of particular interest here, should exploit its biologically active and chiral head group potentially capable to drive the assembly process towards chiral nanostructures. Here we report some spectroscopic and chiroptical data on the reverse micelles formed by DMEB in carbon tetrachloride (CCl_4). A detailed investigation of their ability to confine water in the core of the reverse micelle and of structural features of the assembly are proposed.

In the literature, chiroptical spectroscopies are useful to study chiral surfactants.[4,18–23] The present study is based on

*Correspondence to: S. Abbate, Dipartimento di Medicina Molecolare e Traslazionale, Università di Brescia, Viale Europa 11, 25123 Brescia, Italy. E-mail: abbate@med.unibs.it
Received for publication 6 December 2013; Accepted 23 January 2014

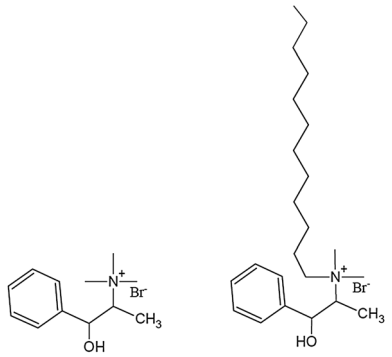

DMEPhe **DMEB**

Scheme 1. Molecular structure of N,N-bis(methyl)-ephedrin bromide (DMEphe) and dodecyl(2-hydroxy-1-methyl-2-phenylethyl)dimethylammonium bromide (DMEB).

the combined use of nuclear magnetic resonance (NMR), Fourier transform infrared (FT-IR), and vibrational circular dichroism (VCD) spectroscopy, as previously reported in the case of reverse micelles of soy lecithin and bis(2-ethylhexyl) sulfosuccinate (AOT) in interaction with dimethyl tartrate molecules.[22,23] To gain insight into the observed VCD features, we added a preliminary Density Functional Theory (DFT) study[24–27] in the present work. The large number of atoms present in DMEB and its high conformational flexibility prompted us to use smaller model compounds with reduced number of atoms and conformations, but still sharing the "ephedra"-like characteristics: (*1R,2S*)-N-methyl-ephedrine (with its enantiomer (*1S,2R*)-N-methyl-ephedrine) (MEPhe), and (*1R,2S*)-N,N-bis (methyl)-ephedrinium bromide (with its enantiomer (*1S,2R*)-N,N-bis (methyl)-ephedrinium bromide) (DMEPhe). DMEPhe was synthesized ad hoc for this work (see Supporting Fig. SI-1a,b) and its structure is reported in Scheme 1 (together with that of DMEB), and in SI-3 of the Supplementary Material. Both enantiomers of MEPhe are commercially available. These two compounds have been studied by VCD as well.

MATERIALS AND METHODS

Materials

DMEB, (*1R,2S*)-MEPhe, and (*1S,2R*)-MEPhe, CCl_4, and $CDCl_3$ were purchased from Sigma-Aldrich and used as received. DMSO-d_6 and D_2O were purchased from Cambridge Isotope Laboratory and used as received.

(*1R,2S*)-N,N-Bis (methyl)-ephedrin bromide and (*1S,2R*)-N,N-bis (methyl)-ephedrin bromide ((*1R,2S*)-DMEPhe and (*1S,2R*)-DMEPhe) were prepared as described in SI-2a and SI-2b of the Supplementary Material.

The deuteration of DMEB is described in SI-2. We noticed that full deuteration of DMEB is difficult to obtain, due to fast hydrogen/deuterium exchange rates.

Methods

All samples were prepared by weight. DMEB/CCl_4 solutions were prepared at various surfactant concentrations ([DMEB] = 0.001, 0.01, 0.05, 0.1 M). Then each water/surfactant/apolar solvent solution was prepared by adding the surfactant/apolar solvent solution to a weighted quantity of water to give the desired water-to-surfactant molar ratio (R = [water]/[DMEB]). It is worth noting that water solubilization in DMEB/CCl_4 solutions is intrinsically a proof of its entrapment in the hydrophilic core of DMEB reverse micelles because its solubility in pure CCl_4 is scarce (0.0075 M).[23] Instead, in 0.1 M DMEB/CCl_4 systems, the water solubility expressed as water to DMEB molar ratio (R) was found to be R = 2.4 at 25 °C.

FT-IR Spectroscopy

FT-IR spectra were acquired at 25 °C with a Spectrum One spectrometer (Perkin Elmer, Boston, MA), using a cell equipped with CaF_2 windows. Each spectrum was the average of eight scans in the 900–4000 cm^{-1} wavenumber range at a spectral resolution of 0.5 cm^{-1}.

VCD Spectroscopy

All VCD experiments were conducted with a Jasco 4000FVS instrument, equipped with two interchangeable detectors, an MCT one used for the mid-IR region (900–1800 cm^{-1}) and an InSb one for the 2000–3200 cm^{-1} region covering, among others, the OD-stretching vibrational modes. The concentrations ranged from 0.1 to 0.2 M. For the preparation of DMEB in CCl_4, a suspension of DMEB was initially heated at 30 °C to make a clear solution. The employed cells had BaF_2 windows and had 200 or 500 μm pathlength, as needed, according to the spectroscopic region and the IR intensities.

DFT Calculations

DFT calculations were performed with the Gaussian09 suite of programs[27] on (1*R*,2*S*)-MEphe and (1*R*,2*S*)-DMEphe with the B3LYP/6-311 + G** functional/basis set choice. Both molecules were treated in vacuo and for DMEphe we considered just the cationic form (without added Br^- counterion). Geometry optimization was obtained after considering the various possible conformers due to the rotational mobility of the OH bond about the CO bond, and caused by relative rotations about the two CC bond connecting the first stereogenic carbon atom C* to the aromatic moiety and to the second stereogenic carbon atom C*. As a matter of fact, we obtained very few conformers (vide infra). Next, harmonic frequencies and dipole and rotational strengths were obtained by the method developed by Stephens[25] and Buckingham *et al.*[26] Lorentzian bandshapes were attributed to each vibrational transition, with bandwidths of 10 cm^{-1} and 16 cm^{-1} in the mid-IR and in the CD/OH stretching regions, respectively.

NMR Spectroscopy

The samples for NMR spectroscopy were prepared in CCl_4 and transferred to 5-mm NMR tubes equipped with a capillary filled with C_6D_6. All the experiments were carried out on a Bruker Avance spectrometer operating at 500 MHz proton frequency. Chemical shifts were referenced to external tetramethylsilane (TMS). Spectral assignments of DMEB were supported by standard 2D methods (COSY, TOCSY). 2D nuclear Overhauser enhancement correlation experiments (NOESY) were acquired by using standard library pulse sequences and at small mixing times to limit spin diffusion effects. The typical settings are detailed in Ref. 23. The diffusion coefficients were measured by pulsed field spin-echo (PGSE) experiments using a pulsed field gradient (PFG) unit capable of producing magnetic field pulse gradients in the z-direction of 53 G · cm^{-1}. The bipolar pulse longitudinal eddy current delay (BPPLED) pulse sequence was used in all the experiments. The duration of the magnetic field pulse gradients (δ) and the diffusion times (Δ) were optimized for each sample to obtain complete dephasing of the signals with the maximum gradient strength. The values of δ and Δ were in the range 2.6–3 and 30–60 ms, respectively. The temperature was set and controlled at 313 K with an air flow of 535 L h^{-1} to avoid any temperature fluctuations due to sample heating during the magnetic field pulse gradients

Samples of water in CCl_4 were prepared by dissolving 10 μL of HPLC grade water in 3 mL of CCl_4.

RESULTS AND DISCUSSION

^{1}H NMR Spectra

The main purpose of the NMR investigation was to draw a picture of the molecular state of water inside the core of the reverse micelles, and to work out the possibility of specific binding of water molecules with the surfactant.

The ^{1}H-NMR experiments were carried out on samples with different water content (R = 1 and 2 water-surfactant molar ratio, see Materials and Methods) and different surfactant concentrations (0.01, 0.1, and 0.2 M). In all cases, water gave a

single peak, thus showing that all the interactions involving the water molecules occurred in the fast exchange dynamic regime on the timescale of NMR spectroscopy. Representative ^{1}H-NMR spectra are reported in SI-4 of SI for R = 1 and [DMEB] = 0.01, 0.1, and 0.2 M. A striking feature is the dramatic change of the resonance frequency of the bound water signal on passing from [DMEB] = 0.01 M to higher concentrations. Indeed, at [DMEB] = 0.01 M the water peak is found at 1.73 ppm, a value deshielded by 0.5 ppm with respect to that observed for water in CCl_4 (see Materials and Methods) at the same temperature, δ = 1.23 ppm (Fig. SI-4). The observed chemical shift of water can be interpreted as the population average between water dispersed in the solvent and water confined in the micellar core. Also, at this low surfactant concentration (at least for NMR spectroscopy), the water resonance indicates a small but appreciable fraction of confined water. In the two cases, [DMEB] = 0.1 and 0.2 M, the water signal was found at 3.55 and 3.76 ppm, respectively. Similar values were found for the samples with R = 2. For these high surfactant concentrations the water molecules are mainly located inside the micellar core.

Experimental proof of the interaction between water and the surfactant molecules was given by nuclear Overhauser enhancement (NOE) correlation experiments, both in the laboratory and rotating frame (NOESY and ROESY, respectively). NOE correlations turned out to be a powerful investigating tool for the assessment of the state of encapsulated molecules within the core of reverse micelles.[28] An example of NOESY spectrum is reported in SI-5. The cross-peaks show the same phase of diagonal peaks, thus indicating slow molecular tumbling. The cross-peak between the water proton and the OH of DMEB indicates direct contact of water molecules with the head of the surfactant, even if no genuine water/surfactant intermolecular NOE was detectable. The chemical exchange nature of the water/OH cross peak was confirmed by ROESY experiments.

Finally, the self-diffusion coefficient of the components of the micellar system were measured. The results are reported in Table 1 and should be interpreted as population-averaged values of free and confined molecules. Without added water (R = 0) the trend of the observed values indicates, as expected, decreasing D with increasing concentration due to the establishment of larger aggregates. For R = 1 and R = 2 the diffusion coefficient of water shows a common feature: for [DMEB] = 0.01 M the observed value D = 3.7 10^{-9} m^2 s^{-1} is independent of the surfactant concentration and matches exactly that of pure water measured in CCl_4 at the same temperature.[29] These results confirm what was discussed above, i.e, at low DMEB concentration water is mainly dispersed in the bulk solvent and in fast exchange with the micellar core on the NMR timescale. By increasing the surfactant concentration, the diffusion coefficient of water decreases by a similar amount for R = 1 and R = 2. Moreover, D (water) and D (surfactant) are on the same order of magnitude, supporting the conclusion of a confinement of water in the micellar core.

TABLE 1. Diffusion coefficients (m^2/s) measured by PGSE-NMR experiments for three different and R = [H_2O]/[DMEB] molar ratios and DMEB concentrations (PGSE = pulsed field gradient spin-echo)

R = 0/ [DMEB]	D (H_2O)	D (DMEB)
0.01 M	—	4.4 10^{-10}
0.1 M	—	3.5 10^{-10}
0.2 M	—	2.7 10^{-10}
R = 1/ [DMEB]		
0.01 M	3.7 10^{-9a}	5.4 10^{-10}
0.1 M	7.3 10^{-10a}	2.0 10^{-10}
0.2 M	4.5 10^{-10a}	1.8 10^{-10}
R = 2/ [DMEB]		
0.01 M	3.7 10^{-9a}	3.8 10^{-10}
0.1 M	6.7 10^{-10a}	2.8 10^{-10}
0.2 M	4.4 10^{-10a}	1.6 10^{-10}

[a]Value corresponding to the population average between free and confined water.

FT-IR Spectra: the OH Stretching Region

Representative spectra of H_2O/DMEB/CCl_4 ([DMEB] = 0.1 M and 0.2 M, R = 0,1,2) solutions in the frequency range 3100-3800 cm^{-1} are shown in Figure 1. The position and width of the OH stretching band (attributable to contributions due to water and/or DMEB) are clear indications of extensive association due to H-bonding. In fact, monomeric alcohols in pure CCl_4 are characterized by a sharp OH stretching band occurring at about 3640 cm^{-1} [30], whereas water monomers dissolved in the same solvent gives two sharp bands due to symmetric and antisymmetric OH stretchings occurring at 3615 and 3708 cm^{-1}, respectively.[31]

OH band of DMEB/CCl_4. In order to gain information on the self-assembling of DMEB in anhydrous conditions, we recorded the spectra of DMEB/CCl_4 solutions at various surfactant concentrations (inset of Fig. 1). Perusal of the DMEB OH stretching bands normalized to the same height of the CH peak at about 2927 cm^{-1} indicates that even at the lowest concentration investigated here (10^{-3}M), the surfactant behaves quite similarly as when the concentrations are higher and surfactant is largely in associated form. Indeed, we found that these bands can be well described by a single Lorentzian peak. It should be noted that by decreasing the surfactant concentration, no significant shift in the band position is observed, but only a small increase in the bandwidth; while a very weak feature at about 3670 cm^{-1}, attributable to monomeric DMEB, appears at the lowest concentrations. The broadening of the band width as well as the appearance of the weak feature can be taken as indications of the clustering of DMEB molecules in smaller aggregates, with just very few DMEB molecules floating around isolated.

OH band of H_2O/DMEB/CCl_4. The evolution of the OH band with increasing R value is shown in Figure 1. It can be noted that water addition involves an increase of the intensity of the

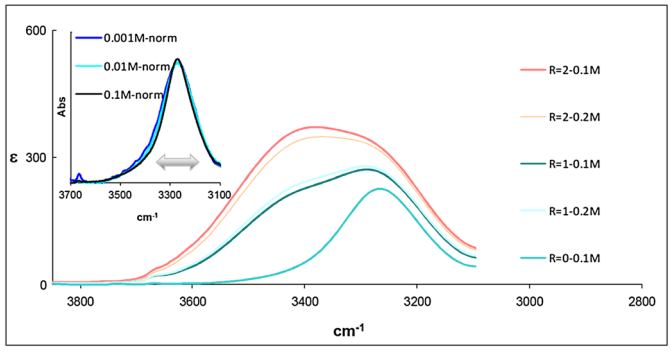

Fig. 1. IR spectra of DMEB in CCl_4 (R = 0) and H_2O/DMEB/CCl_4 (R = 1 and R = 2). Inset: Normalized IR spectra of DMEB in CCl_4 (concentration range from 10^{-3} to 0.1 M). ε was calculated using the DMEB concentration.

band at about 3271 cm^{-1} as well as the appearance of a new contribution at about 3440 cm^{-1}. By comparing with the data in the absence of water, the 3271 cm^{-1} component is attributed to OH-stretching of DMEB molecules, whereas the 3440 cm^{-1} contribution can be attributed to OH stretching of clustered water molecules, which are confined within the core of DMEB reverse micelles. This assumption is still tentative and will be compared with the conclusions based on VCD in the OD stretching region. We also considered deconvolution of all bands in the OH stretching region, finding that they can be well described by two Gaussian components (fitting parameters are reported in SI-6). For the sake of comparison, the fitting parameters of the three Gaussian components of the bulk water OH stretching band are also reported.[32]

In SI-6 we observe that the component at about 3440 cm^{-1}, attributable to confined water, and the component at about 3270 cm^{-1}, attributable to DMEB OH stretchings plus some contributions from water, exhibit a redshift and some broadening with R. This behavior suggests that water addition involves the buildup of more hydrogen bonded structures accompanied by an increase of their structural variety. This is also consistent with the hypothesis that while at the lowest R values water molecules are hydrogen bonded with the DMEB OH group, water–water interactions may occur at higher R. All this will have an interesting counterpart in the deuterated molecules IR and VCD spectra (vide infra), as well as in the NMR spectra. Comparing the fitting parameters of bulk water OH stretching, it can be also concluded that while the component at 3595 cm^{-1} is absent, the components at 3314 and 3460 cm^{-1} are redshifted by 41–44 and 6–26 cm^{-1}, respectively. The existence of such redshifts and the absence of the 3595 cm^{-1} component may be taken as an indication that the structural arrangement of water molecules confined in the DMEB reverse micelles is significantly different from that of bulk water.

FT-IR and VCD Spectra: The Mid-IR Region

The IR and VCD spectra in the mid-IR region are reported in Figure 2 for CCl_4 0.1 M solutions of DMEB and DMEB-d_1 per se and with H_2O or D_2O, respectively (cases R = 0, 1, and 2). VCD, which has been established through the years as a powerful and reliable tool for configurational assignment together with DFT calculations,[24–26,33–38] was also applied to study reverse micelles.[22,23,39] It is also worth mentioning that VCD spectra for ephedra molecules had already been presented in the CH-stretching region.[40] In the SI file one may find our mid-IR VCD spectra of one of the ephedra molecules studied in previously[40] (MEPhe), whose mid-IR spectra was also presented[41]: in the SI we compare the VCD spectra of MEPhe and DMEB. For both DMEB and DMEB-d_1, there is no evidence of variation in the IR and VCD bands with increasing R. This region is less informative or, at least, does not provide direct evidence, as above, for the study of DMEB molecules ability to host D_2O or H_2O in the interior of the reverse micelles.

However, a few facts are worth observing in the 900–1180 cm^{-1} region, which are of some importance in subsequent analysis. Both in the IR and VCD spectra one may notice the decrease of the intensity of the feature at 1053 cm^{-1}, which is blueshifted by 10 cm^{-1} when one moves from DMEB to DMEB-d_1. This is accounted for also by the DFT calculations of DMEPhe allowing attributing this feature to OH (OD) bending coupled to CH_3-C*H stretching. This behavior is also accompanied by new positive features at 1074 and 1103 cm^{-1} (on the basis of DFT calculations, assigned to deformation modes of methyl groups of CH bendings of the phenyl groups, with minor contributions from OD bending) in the VCD spectra of the deuterated molecules. Other changes in the VCD spectra can be noted: at ca. 1250 cm^{-1} a positive VCD feature decreases significantly from DMEB to DMEB-d_1; some other minor changes appear at 1400 cm^{-1} and at 1470/1500 cm^{-1}.

The above changes are accounted for by the DFT calculations for DMEPhe and DMEPhe-d_1 (see Fig. 2). In Supplementary Information (SI-7 and SI-8) we provide calculated structures and calculated IR and VCD spectra for (1*R*,2*S*)-DMEPhe, as well as for the more common methyl ephedrine (1*R*,2*S*)-MEPhe (see Refs. 40,41). Due comparison with the

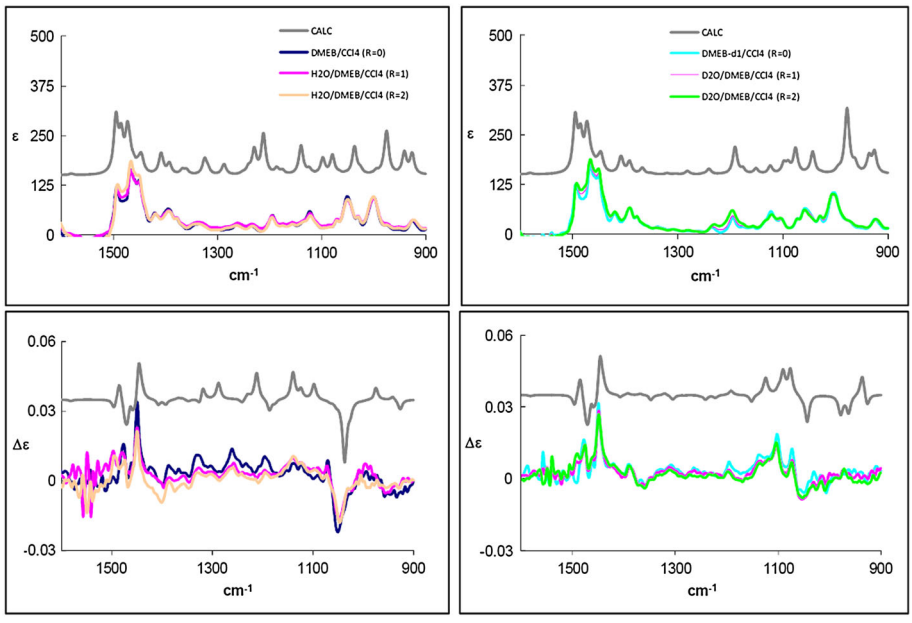

Fig. 2. Experimental IR and VCD spectra of DMEB in CCl_4 (R = 0) and H_2O/DMEB/CCl_4 (R = 1 and R = 2) (left panels); IR and VCD spectra of DMEB-d_1 in CCl_4 (R = 0) and D_2O/DMEB/CCl_4 (R = 1 and R = 2) (right panels). Calculated spectra for DMEPhe (left panels) and deuterated DMEPhe (right panels) in vacuo are also reported. ε and Δε were calculated using the DMEB concentration.

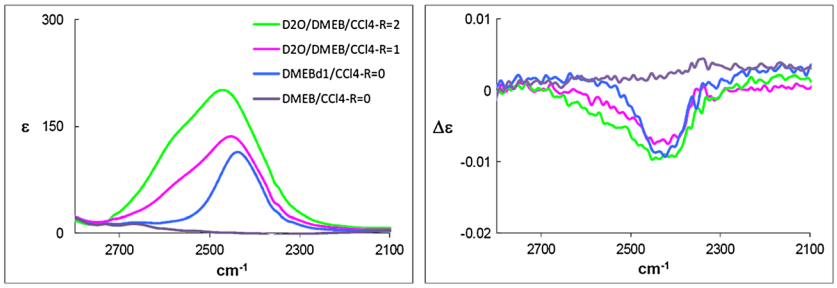

Fig. 3. Experimental IR and VCD spectra of DMEB-d_1 in CCl_4 (R = 0) and D_2O/DMEB/CCl_4/ (R = 1 and R = 2). ε and Δε were calculated using the DMEB concentration.

corresponding experimental spectra of both enantiomers in solution is provided there. The reader may appreciate the similarities with the spectra of DMEB. However, the DMEPhe spectra could be taken just in DMSO-d_6 and no other solvent assured enough solubility to conduct VCD spectroscopy. DFT calculations in vacuo permit almost full understanding of VCD and IR spectra of MEPhe (Fig. SI-8) (cf. Refs. 40,41]). This molecule presents two conformers: the most populated one (87%) with an OH…N intramolecular hydrogen bond and the other one (13%) with a free OH group. DMEphe has just one populated conformer with the OH group free from intramolecular hydrogen bonding (see SI-7). For (1*R*,2*S*)-DMEPhe, which is more relevant for our investigation of the surfactant properties of DMEB, a characteristic (+ - +) VCD triplet is observed between 1500 and 1450 cm^{-1} and is explained by the calculated features at 1525, 1510, and 1485 cm^{-1}: associated normal modes are mainly due to the trimethyl-ammonium group with contributions also from phenyl in-plane CH bendings. Below 1400 cm^{-1} the DMEPhe spectra are strongly perturbed by the solvent. The in vacuo calculations show instead an acceptable correspondence with the experiments of DMEB in CCl_4, as presented in Figure 2: some contributions from OH or OD bending is noticed for the lower frequency features and have been used to explain the variability in the VCD data from DMEB to DMEB-d_1.

The presence or absence of either H_2O or D_2O does not significantly affect spectra, within the error limits of our experiments. This fact, together with the good prediction of data through the calculations for the isolated molecule (either in the hydrogenated or deuterated form) brings us to conclude, that, in this case, VCD in the mid-IR is almost insensitive to the presence of a few water molecules. Anyway, as expected, the data show high sensitivity to deuteration of the hydroxyl group in DMEB.

FT-IR and VCD Spectra; The OD-Stretching Region

To exploit the good sensitivity of our apparatus in the OD stretching region, we studied DMEB-d_1. In Figure 3 we report the IR and VCD spectra in the 2150–2800 cm^{-1} region for DMEB and DMEB-d_1 in CCl_4 neat solution (R = 0) and in CCl_4 solution with addition of D_2O (R = 1 and 2); this region contains contributions from OD stretching normal modes. Indeed, one may notice one fairly strong absorption band centered at ca. 2440 cm^{-1}, which moves to 2480 cm^{-1} with addition of D_2O and with an increasingly more evident shoulder at ca. 2600 cm^{-1}. The latter shoulder appears to be proportional to the D_2O content, while spectra, reported in ε, are independent of the DMEB-d_1 concentration, within the range 0.1–0.2 M (data not shown).

Correspondingly, the VCD spectra show a negative band centered at 2435 cm^{-1} which is slightly blueshifted with increasing R. The VCD band is slightly but evidently asymmetric and presents a negative shoulder at ca. 2600 cm^{-1}, which grows with R. (The instrumental setting for the VCD data in this region has been optimized by running the VCD spectra in the CD-stretching region for (*3R*)-methyl cyclopentanone-d_4.[42]) In parallel with the findings of the IR spectra in the first part of this article, we assign the lower frequency feature (ca. 2440 cm^{-1}) to the OD stretching of DMEB-d_1 involved in hydrogen (deuterium) bonding in the core of DMEB-d_1 micelles.

The fact that the VCD signal in Δε units does not increase in parallel with absorption in ε units with increasing D_2O content and is centered at 2440 cm^{-1} further supports that this feature is due to the OD-stretching of DMEB-d_1. Its vibrational optical activity is due to the OD being close to the chiral center of DMEB-d_1. Instead, the strong IR shoulder at 2600 cm^{-1} is due to D_2O and corresponds to a much less prominent shoulder in VCD; this leads us to conclude that the OD stretchings of D_2O show some vibrational optical activity. Some backup to this assignment comes from quite preliminary DFT calculations of the OH and OD stretching region of DMEPhe and DMEPhe-d_1, respectively. The results are for the isolated molecules or for complexes with two DMEPhe (DMEPhe-d_1) with one H_2O (D_2O) molecule between the two. The structures for the optimized geometries of the complex are reported in Figure SI-9, while the calculated absorption spectra in the OH- and OD-stretching region are given in Figures SI-10 and SI-11, respectively (bands have been shifted assuming an anharmonicity constant $\chi = 80\ cm^{-1}$ for OH and, as a consequence, $\chi = 40\ cm^{-1}$ for OD[43,44]). Two facts emerge from these preliminary results: first, the OH (OD) stretching is predicted to have an unusually high frequency for the surfactant molecule in isolation, namely, 3811 cm^{-1} (2694 cm^{-1}). Second, the interaction of two DMEPhe-d_1 molecules through a water bridge with D_2O brings the OD stretching frequency of DMEPhe-d_1 close to the experimentally recorded values, with higher IR and VCD intensity with respect to the deuterated hydroxyl in the isolated molecule and with correct VCD sign. Both facts have a nice correspondence with the observed data of DMEB-d_1. A complete explanation of the observed VCD signal associated with OD-stretchings of D_2O would require a more complete approach encompassing a detailed statistical analysis of more complex systems with many possible geometries.

CONCLUSION

In this work we investigated some spectroscopic properties of the chiral surfactant molecule DMEB in apolar solvents. NMR permitted establishing that DMEB forms aggregates

bearing the properties of reverse micelles, with trapped water molecules quite close to the polar heads of DMEB. FT-IR spectroscopy confirms this view, but further allows to establish, in highly diluted solutions, the presence of a few isolated DMEB molecules through the observation of high wavenumber OH stretching signal.

Finally, VCD has also confirmed these findings with the addition that self-assembled DMEB molecules are organized such that the OH (OD) bonds show a nice negative vibrational optical activity feature. Trapped water (deuterium oxide) possesses just a modest negative vibrational optical activity. Then, together with NMR, VCD indicates the presence of system-specific water-head groups interactions. As already found in the literature[4] and based on the present study, we conclude that DMEB is an ideal surfactant molecule to evidence chiral-specific interactions, and this is due to one of the stereogenic carbon atoms being quite close to the polar head of DMEB. In fact, from the OD-stretching region of the IR and VCD spectra we have gathered some evidence of a specific interaction between DMEB-d_1 and D_2O: on the higher frequency side of the strong negative VCD band recorded also in absence of D_2O, assigned to the OD stretching of DMEB-d_1, we observe a shoulder associated with the OD-stretching of D_2O. This fact hints at a chiral arrangement of D_2O molecule (s). The calculations presented in SI are encouraging but very preliminary; future work will be devoted to a systematic statistical analysis on larger DMEB-d_1/D_2O complexes.

ACKNOWLEDGMENT

We thank the Computing Center CINECA Via Magnanelli 6/3 40033 - Casalecchio di Reno (Bologna) Italy for access to their computational facilities.

SUPPORTING INFORMATION

Additional supporting information may be found in the online version of this article at the publisher's web-site.

LITERATURE CITED

1. Rosen MJ. Surfactants and interfacial phenomena, 1st ed. New York: John Wiley & Sons; 1978.
2. Colombo LM, Thomas RM, Luisi PL. Chirality of reverse micelles. Chirality 1991;3:233–241.
3. Xia J, Nnanna IA, Sakamoto K. Amino acids surfactants: chemistry, synthesis, and properties. In: Nnanna IA, Xia J, editors. Protein-based surfactants: synthesis, physiochemical properties and applications. Surfactant Science Series Vol. 101. New York: Marcel Dekker; 2001. p 75–122.
4. Sorrenti A, Altieri B, Ceccacci F, Di Profio P, Germani R, Giansanti L, Savelli G, Mancini G. Deracemization of bilirubin as the marker of the chirality of micellar aggregates. Chirality 2012;24:78–85.
5. Pahi AB, Varga D, Kiraly Z, Mastalir A. thermodynamics of micelle formation of the ephedrine-based chiral cationic surfactant DMEB in water, and the intercalation of DMEB in montmorillonite. Coll Surf A Physicochem Eng Asp 2008;319:77–83.
6. Roy S, Khatua D, Dey J. Giant vesicles of a single-tailed chiral cationic surfactant, (1R, 2S)-(-)-N-dodecyl-N-methyl-ephedrinium bromide in water. J Coll Int Sci 2005;292:255–264.
7. Fireman-Shoresh S, Popov I, Avnir D, Marx S. enantioselective, chirally templated sol – gel thin films. J Am Chem Soc 2005;127:2650–2655.
8. Feng Z, Li Y, Niu D, Li L, Zhao W, Chen H, Li L, Gao J, Ruanb M, Shi J. A facile route to hollow nanospheres of mesoporous silica with tunable size. Chem Commun 2008;2629–2631.
9. Gübitz G, Schmid MG. Recent progress in chiral separation principles in capillary electrophoresis. Electrophoresis 2000;21:4112–4135.
10. Dey J, Mohanty A, Roy S, Khatua D. Cationic vesicles as chiral selector for enantioseparations of nonsteroidal antiinflammatory drugs by micellar electrokinetic chromatography. J Chromatogr A 2004;1048:127–132.
11. Bunke A, Jira T, Beyrich T. (–)-N-Dodecyl-N-ephedrinium bromide as chiral selector in capillary electrophoresis. Pharmazie 1997;52:762–764.
12. Colonna S, Re A, Wynberg H. Asymmetric induction in the Michael reaction by means of chiral phase-transfer catalysts derived from cinchona and ephedra alkaloids. J Chem Soc Perkin Trans 1981;1:547–552.
13. Wu W, Zhang Y. Enantioselective synthesis of α-amino acids in chiral reverse micelles. Tetrahedron Asymmetry 1998;9:1441–1444.
14. Fletcher PDI, Galal MF, Robinson BH. Structural study of AOT stabilised microemulsions of glycerol dispersed in n-heptane. J Chem Soc Faraday Trans 1 1984;80:3307–3314.
15. Arcoleo V, Aliotta F, Goffredi M, La Manna G, Turco Liveri V. Study of AOT-stabilized microemulsions of formamide and n-methylformamide dispersed in n-heptane. Materials Sci Eng C 1997;5:47–53.
16. Gomez-Herrera C, Del Mar Graciani M, Munoz E, Moya ML, Sanchez F. Kinetics of the oxidation of iodide by peroxodisulphate in reverse micelles. J Coll Int Sci 1991;141:454–458.
17. Zhang R, Liu J, Han B, He J, Liu Z, Zhang J. Recovery of nanoparticles from $(EO)_8(PO)_{50}(EO)_8$/p-Xylene/H_2O microemulsions by tuning the temperature. Langmuir 2003;19:8611–8614.
18. Polavarapu PL, Vijay R. Chiroptical spectroscopy of surfactants. J Phys Chem A 2012;116:5112–5118.
19. Vijay R, Baskar G, Mandal AB, Polavarapu PL. Unprecedented relationship between the size of spherical chiral micellar aggregates and their specific optical rotations. J Phys Chem A 2013;117:3791–3797.
20. Vijay R, Polavarapu PL. FMOC-amino acid surfactants: discovery, characterization and chiroptical spectroscopy. J Phys Chem A 2012;116:10759–10769.
21. Novotná P, Urbanová M. Vibrational circular dichroism study of polypeptide model-membrane systems. Anal Biochem 2012;427:211–218.
22. Abbate S, Longhi G, Ruggirello A, Turco Liveri V. Confinement of chiral molecules in reverse micelles: FT-IR, polarimetric and VCD investigation on the state of dimethyl tartrate in sodium bis(2-ethylhexyl) sulfosuccinate reverse micelles dispersed in carbon tetrachloride. Coll Surf A Physicochem Eng Aspects 2008;327:44–50.
23. Abbate S, Castiglione F, Lebon F, Longhi G, Longo A, Mele A, Panzeri W, Ruggirello A, Turco Liveri V. Spectroscopic and structural investigation of the confinement of D and L dimethyl tartrate in lecithin reverse micelles. J Phys Chem B 2009;113:3024–3033.
24. Stephens PJ, Devlin FJ, Cheeseman JR. VCD spectroscopy for organic chemists. New York: CRC Press; 2012.
25. Stephens PJ. Theory of vibrational circular dichroism. J Phys Chem 1985;89:748–752.
26. Buckingham AD, Fowler PW, Galwas PA. Velocity-dependent property surfaces and the theory of vibrational circular dichroism. Chem Phys 1987;112:1–14.
27. Gaussian 09, Revision A.02, Frisch MJ, Trucks GW, Schlegel HB, Scuseria GE, Robb MA, Cheeseman JR, Scalmani G, Barone V, Mennucci B, Petersson GA, Nakatsuji H, Caricato M, Li H, Hratchian HP, Izmaylov AF, Bloino J, Zheng G, Sonnenberg JL, Hada M, Ehara M, Toyota K, Fukuda R, Hasegawa J, Ishida M, Nakajima T, Honda Y, Kitao O, Nakai H, Vreven T, Montgomery JA Jr, Peralta JE, Ogliaro F, Bearpark M, Heyd JJ, Brothers E, Kudin KN, Staroverov VN, Kobayashi R, Normand J, Raghavachari K, Rendell A, Burant JS, Iyengar SS, Tomasi J, Cossi M, Rega N, Millam JM, Klene M, Knox JE, Cross JB, Bakken B, Adamo C, Jaramillo J, Gomperts R, Stratmann RE, Yazyev O, Austin AJ, Cammi R, Pomelli C, Ochterski JW, Martin RL, Morokuma K, Zakrzewski VG, Voth GA, Salvador P, Dannenberg JJ, Dapprich S, Daniels DD, Farkas, Foresman JB, Ortiz JV, Cioslowski J, Fox DJ, Gaussian, Inc.: Wallingford CT; 2009.
28. Crans, DC, Rithner CD, Baruah B, Gourley BL, Levinger NE. Molecular probe location in reverse micelles determined by NMR dipolar interactions. J Am Chem Soc 2006;128:4437–4445.
29. Holz M, Heila SR, Sacco A. Temperature-dependent self-diffusion coefficients of water and six selected molecular liquids for calibration in accurate ^{1}H NMR PFG measurements, Phys Chem Chem Phys 2000;2:4740–4742.
30. Wilson L, Bicca de Alencastro R, Sandorfy C. Hydrogen bonding of n-alcohols of different chain lengths. Can J Chem 1985;63:40–45.
31. Kuo M, Kamelamela N, Shultz MJ. Rotational structure of water in a hydrophobic environment: carbon tetrachloride. J Phys Chem A 2008;112:1214–1218.

32. Calandra P, Caponetti E, Chillura Martino D, D'Angelo P, Minore A, Turco Liveri V. FT-IR and dielectric study of water/AOT liquid crystals. J Mol Struct 2000;522:165–178.
33. Nafie LA. Vibrational optical activity, principles and applications. Hoboken, NJ: John Wiley & Sons; 2011.
34. Stephens PJ, Devlin FJ, Pan JJ. The determination of the absolute configurations of chiral molecules using vibrational circular dichroism (VCD) spectroscopy. Chirality 2008;20:643–663.
35. Taniguchi T, Miura N, Nishimura S, Monde K. Vibrational circular dichroism: chiroptical analysis of biomolecules. Mol Nutr Food Res 2004:48:246–254.
36. Polavarapu PL. Renaissance in chiroptical spectroscopic methods for molecular structure determination. Chem Rec 2007;7:125–136.
37. Yang G, Xu Y. Vibrational circular dichroism spectroscopy of chiral molecules. In: Nauman R, Beratan DN, Waldeck DH, editors. Electronic and magnetic properties of chiral molecules and supramolecular architectures. Berlin, Heidelberg: Springer; Top Curr Chem 2011;298:189–236.
38. Brizard A, Berthier D, Aimé C, Buffeteau T, Cavagnat D, Ducasse L, Huc I, Oda R. Molecular and supramolecular chirality in gemini-tartrate amphiphiles studied by electronic and vibrational circular dichroism. Chirality 2009;21:E153–162.
39. Abbate S, Gangemi R, Lebon F, Longhi G, Passarello M, Ruggirello A, Turco Liveri V. Investigations of methyl lactate in the presence of reverse micelles by vibrational spectroscopy and circular dichroism. Vibration Spectrosc 2012;60:54–62.
40. Freedman TB, Ragunathan N, Alexander S. Vibrational Circular dichroism in ephedra molecules. Experimental measurement and ab initio calculation. Faraday Discuss 1994;99:131–149.
41. VCD spectrum posted on BioTools, Inc. Website: http://www.btools.com; Jupiter, FL.
42. Gangemi R, Longhi G, Lebon F, Abbate S, Laux L. Vibrational excitons in CH-stretching fundamental and overtone vibrational circular dichroism spectra. Monatsh Chem 2005;136:325–345.
43. Gangemi F, Gangemi R, Longhi G, Abbate S. Experimental and ab-initio calculated VCD spectra of the first OH-stretching overtone of (1R)-(-) and (1S)-(+)-endo-borneol. Phys Chem Chem Phys 2009;11:2683–2689.
44. For the relation used in text: $\chi_{OD} = (1/2)\chi_{OH}$, refer to a general text on Vibrational Spectroscopy reporting anharmonicity constants in the case of anharmonic oscillators.